Heliyon 10 (2024) e24663

Contents lists available at ScienceDirect

Heliyon

journal homepage: www.cell.com/heliyon

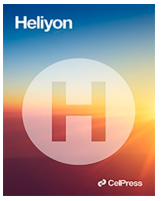

Research article

Tracking flowpaths in a complex karst system through tracer test and hydrogeochemical monitoring: Implications for groundwater protection (Gran Sasso, Italy)

V. Lorenzi [a], F. Banzato [b], M.D. Barberio [c,*], N. Goeppert [d], N. Goldscheider [d], F. Gori [a], A. Lacchini [a], M. Manetta [a], G. Medici [a], S. Rusi [e], M. Petitta [a]

[a] Earth Science Department, Sapienza University of Rome, Italy
[b] Autorità di Bacino Distretto Idrografico Appennino Centrale, Italy
[c] National Institute of Geophysics and Volcanology, Rome, Italy
[d] Institute of Applied Geosciences, Division of Hydrogeology, Karlsruhe Institute of Technology (KIT), Karlsruhe, Germany
[e] Engineering and Geology Department, University G. D'Annunzio, Chieti, Italy

ARTICLE INFO

Keywords:
Groundwater
Karst aquifer
Tracer test
Isotope
Flowpaths

ABSTRACT

Groundwater in karst aquifers is frequently tapped for drinking purposes, due to frequent huge volumes of resources. Unfortunately, vulnerability of these aquifers can be high, due to possible fast transfer of recharge water on springs by the karst network. On Gran Sasso Mountain regional aquifer, several springs are subjected to drinking withdrawal and an updated evaluation of their potential is now a fundamental issue to be considered, facing climate change effects, which reflect on variation of discharge regimen and values. To distinguish between different contribution of spring recharge, a tracer test has been carried out on the Vitella d'Oro spring, fed both by the regional aquifer and by a local system exposed to karst features developed in the Rigopiano Conglomerates formation. Thanks to hydrogeological, hydrogeochemical and isotopic data, a conceptual model of spring recharge has been proposed and subsequently validated by the tracer test results. All information confirms the superimposition on the regional base flow, by a relevant contribution of the karst network, influencing the spring discharge in recharge periods. In detail, a fast flow component is responsible for discharge peaks and frequently of turbidity events, having a mean velocity ranging from 30 to 70 m/h in the aquifer. Besides of this fast flow, an additional aliquot of the recharge is due to the same local aquifer, but slower flow clearly identifiable by hydrochemistry and isotopic data. Thanks to these findings, a renewed management of the spring has been suggested, considering the different degrees of aquifer vulnerability (turbidity occurrence) directly related to the discharge regimen.

1. Introduction

Among aquifer systems, karst environments represent those with the most complex groundwater hydrodynamics. Despite karst aquifers cover only 15% of global continental areas, they are one of the main resources of fresh water for human use and for drinking purpose [1–6]. In particular, based on a careful global evaluation in 2016, 678 million people used karst water [4]. This type of

* Corresponding author.
E-mail address: marinodomenico.barberio@ingv.it (M.D. Barberio).

https://doi.org/10.1016/j.heliyon.2024.e24663
Received 25 July 2023; Received in revised form 11 January 2024; Accepted 11 January 2024
Available online 14 January 2024

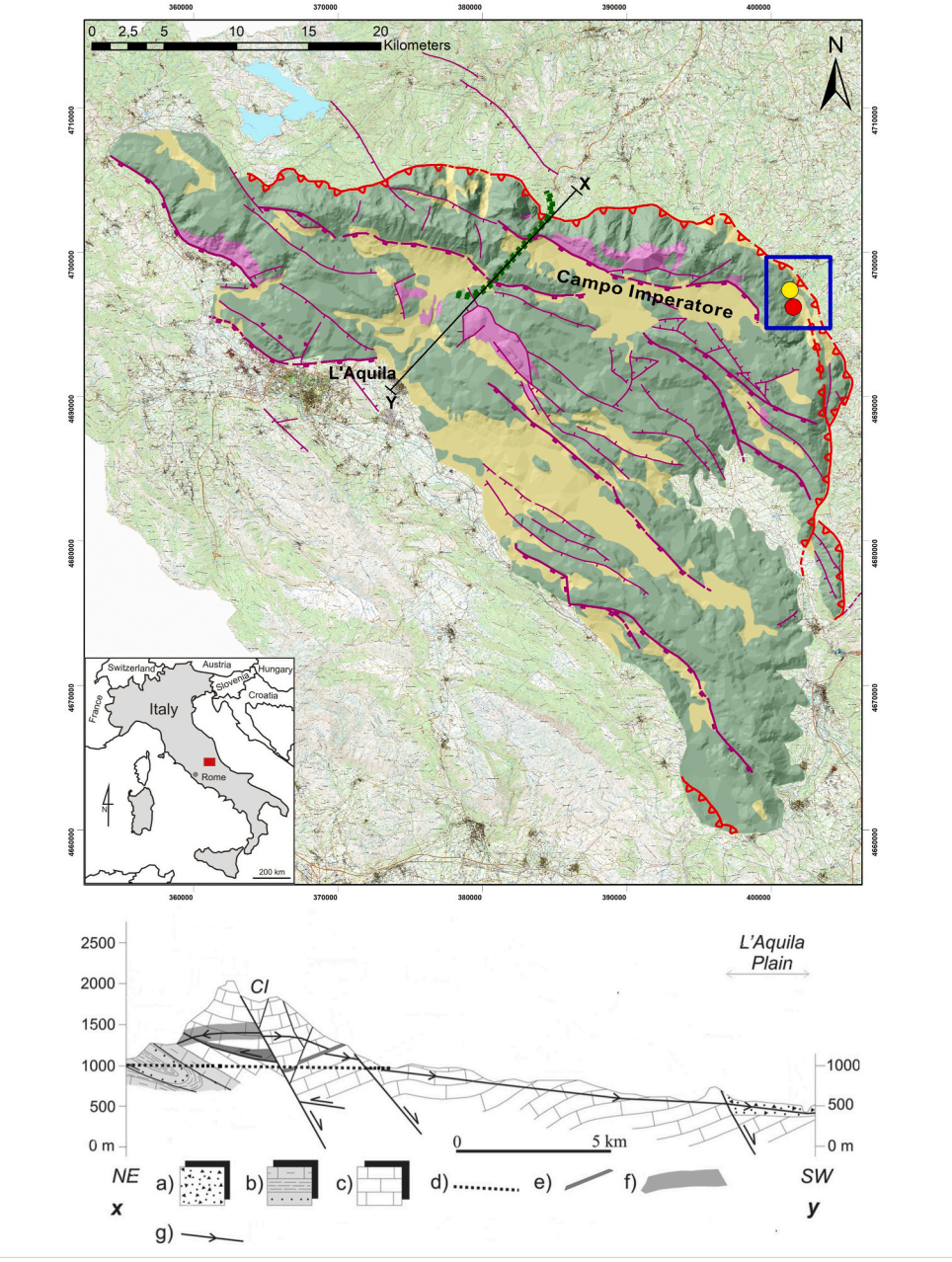

(caption on next page)

Fig. 1. Simplified hydrogeological setting of the Gran Sasso aquifer. The Tavo spring group includes Vitella d'Oro and Mortaio d'Angri springs (modified from 57). Below: Conceptual groundwater flow model (modified by 57). a Quaternary aquitard; b upper Miocene aquiclude; c regional carbonate aquifer (Miocene—Upper Triassic); d highway tunnels; e local aquiclude; f karst horizon; g water table; CI: Campo Imperatore. The blue rectangle corresponds to the study area, displayed in detail in Fig. 3.

groundwater system differs substantially from the porous and fissured aquifers. In the latter ones, permeability, porosity, transmittivity, and hydraulic gradient play a fundamental role in governing the direction and flow dynamics [1,7–9]. In karst systems also other factors must be taken into account. Indeed, dissolution processes, tectonic discontinuities, and deep fluid upwelling [10–13] define peculiar features in the hydrogeological systems. In fact, the development of conduits and caves make the groundwater hydrodynamics temporally and spatially variable [11,14–20]. In this context, the water flow can reach a velocity up to several hundred m/h [21]. This behaviour can favour the dispersion of potential pollutants, due to reduced self-cleaning capacity through the fast flow from recharge to discharge area [22,23]. Additionally, other factors such as over-exploitation [22], and climate change [13,24,25] make groundwater a vulnerable resource in karst. In order to protect and manage the water resource from human activity, in many cases the government institution adopted preventive measures (e.g., land use restrictions in protected areas) [21,26,27]. In the last decades, many studies focusing on groundwater flow in karst systems are growing to better understand their complex hydrodynamics [10]. The main methodological approach consists of the application of both natural and artificial tracers [28–31] with the aim of separating the water contribution of flows with different velocities and directions. This method is also considered the best one for delineating the catchment area of karstic springs [20,32,33]. Natural tracers consist of substances that commonly occur in environments. They include inorganic and organic chemical materials, and stable and radioactive water isotopes (^{2}H, ^{3}H, and ^{18}O), that are the most used for assessing groundwater age and defining recharge area [3,34–41]. On the other hand, artificial tracers (e.g., fluorescent dyes) are used to in-depth characterize groundwater flow and contaminant transport [21,30,39,41–44].

In order to characterize the groundwater hydrodynamics of the Gran Sasso karst aquifer, we investigated in detail the north-eastern sector of this aquifer system, due to the processes of springs tapped for drinking purposes.

Hydrogeochemical monitoring has been performed at the Tavo spring group since 2021, the Vitella D'Oro and the Mortaio D'Angri springs, which are part of the same aqueduct system. Besides, in April 2022 a tracer test has been realised to better understand the hydrodynamic and the hydrogeology of the karst circuits. Both hydrogeochemical and tracer test results shed light on the presence of two different recharge areas that feed the two springs. In detail, the Vitella d'Oro spring is characterised by a relatively complex groundwater basin due to the presence of karst networks and karst conduits, whose contributions are more evident during intense meteoric events.

Since the sensitiveness of the Vitella d'Oro spring to scale discharge/recharge variations, this study aims to assess different flowpaths of the two Tavo springs in order to optimize the management and preservation of groundwater. In detail, the main research questions to be faced are related to: i) the influence of karst network on the spring recharge, in terms of time-transfer and discharge amount; ii) the sensitivity to extreme events and consequent trigger of turbidity in the spring outlet; iii) the assessment of the common and different recharge areas for both spring.

2. Geological and hydrogeological settings

During the Oligocene-Quaternary period, the central Apennines fold-thrust belt was developed. It is characterised by a main eastward vergence and a classical foreland-ward propagation of thrust faults. The compressional phase was followed by the Tyrrhenian back-arc extension [45–52]. Due to the slab retreat of the Adriatic plate, the central Apennines have moved eastward to the European plate since Oligocene period [46,51,53,54]. During the Quaternary, the evolution of the Apennine was characterised by an extensional regime and influenced by thick sequence of continental deposits [55,56]. Moreover, in the Plio-Quaternary tectonics period, the clastic and alluvial deposits filled the intramontane plains [46,55,56]. It affected groundwater circulation within the karst aquifers, by hindering the evolution of the karst system. In fact, the sedimentation rate and fault activities have caused variations in the groundwater level of the aquifer, preventing the classical development of karst network [57]. Thus, karst evolution provides high infiltration rate and huge groundwater resources, while springs fed by groundwater flow coming from the fracture network, are defined by a steady regimen [55]. It follows that groundwater flow is concentrated toward springs, situated at the border of the aquifer,

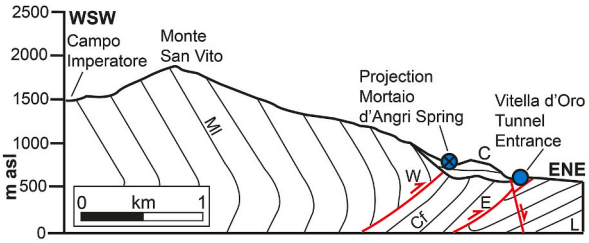

Fig. 2. Simplified geological cross-section (modified from 66) showing the easternmost (E) and westernmost (W) thrusts, one of the normal post-orogenic faults, and the multiple hydrogeological units that characterize the study site: Complex of the Mesocenozoic limestones (Ml), and the geological formations of the Monte dei Fiori Calcarenites (Cf), Laga Formation (L), and the Rigopiano Conglomerates (C).

characterised by a seasonal response to recharge [58].

Vitella d'Oro and Mortaio d'Angri springs are located in the proximity of the two thrusts that characterize the easternmost sector of the Gran Sasso Massif (Fig. 1).

From a structural point of view, the outcropping rocks are heavily fractured by the effects of either the compressional or extensional tectonics in the Tavo Valley. Here, two major thrusts and the axes of the associated overturned folds are NW-SE oriented (Fig. 1; [59–62]). The Mortaio d'Angri spring is located in correspondence with the thrust between the Montefiore Calcarenites Formation, and the highly permeable and karstified Meso-Cenozoic limestones which represent the main regional aquifer [63,64]. The tectonic contact mapped in correspondence with the Mortaio d'Angri spring is the westernmost thrust that characterizes the study site (Figs. 1 and 2). 1.5 km north-east with respect to Mortaio d'Angri is located at the entrance of the tunnel draining Vitella d'Oro Spring (Fig. 2). The emergence of the Vitella d'Oro tunnel is closeby the easternmost thrust between the Montefiore Calcarenites aquifer with the aquitard of the Laga Formation (Fig. 2). It is noteworth that Messinian gypsum that easily dissolves is present at the footwall of the easternmost thrust and is stratigraphically part of the Laga Formation of Messinian age [65,66]. No contact between the thrust and the evaporates is established by the footwall synclines; instead, the contact is due to the presence of an extensional fault [61]. In this heavily tectonized sector of the study site, the gypsum mineral species with potential source from the evaporitic deposits can be found as seal of extensional related fractures (see the cross section in Fig. 2). The stratigraphic succession is heavy folded and the beds at either the hangingwall or the footwall of the easternmost thrust dip between 30° and 70° (Fig. 2). Of note, a geological formation of Early Pliocene age (Rigopiano Conglomerates) is 0°–30° dipping and is placed above an erosional unconformity that divides these coarse-grained siliciclastic sediments from the deposits of marine sedimentary origin of Cretaceous to Miocene age (Fig. 2). The conglomerates show a pelitic matrix, and are characterised by clasts of cherts, dolostones, limestones, quartz and feldspars [51,61,65]. These conglomerates are of paramount importance for the local hydrogeology: the tunnel of the Vitella d'Oro spring is directly draining these deposits overlapping the second thrust (Fig. 2), and consequently, they represent the main recharge area of the spring.

From a geomorphological point of view, large karst landforms such as dolines of several meters are absent at the study site, but they are very frequent in the Campo Imperatore area, although cavities with diameters up to 0.30 m have been found in the recharge area of the springs. However, in the subsurface, karst conduits with diameters up to 1.0 m are frequent in the Rigopiano Conglomerates formation [64,67], revealing a local karst input on the Vitella d'Oro spring.

The Gran Sasso karst aquifer (Abruzzi region, central Italy) is 1034 km^2 wide and it is one of the largest karst aquifers of the central Apennines. This area is relevant for the huge availability of groundwater resources for human purposes [68] but also for problems related to the Gran Sasso motorway tunnel [63,69–73]. Moreover, the karst aquifer is located within a National Park, highlighting the importance of satisfying human and ecosystem requirements [74].

Along the northern side, the Gran Sasso carbonate aquifer is bounded by Miocene flysch (terrigenous units) that represents the regional aquiclude. Along its southern side, the aquifer is bounded by Quaternary continental deposits, acting as the regional aquitard

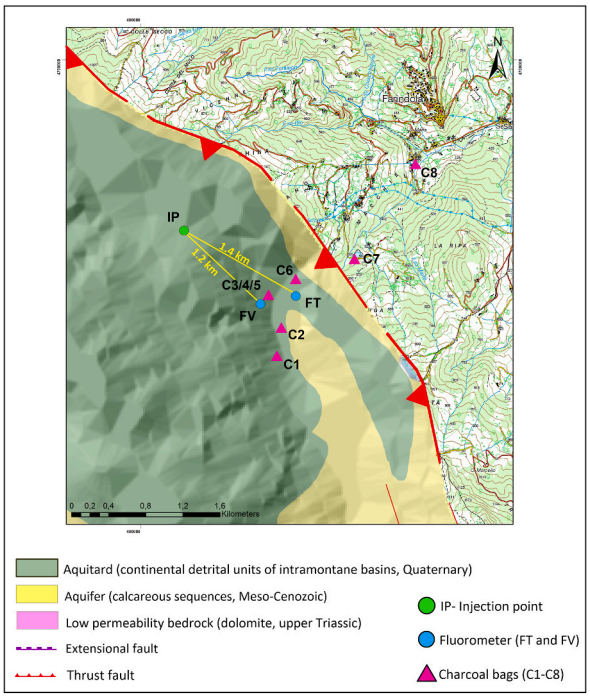

Fig. 3. On the left, location of the injection point (IP) and of the two tracer monitoring points (FT: Fluorometer at Tavo River, and FV: Fluorometer at the Vitella d'Oro tunneling). On the right, location of FT and FV with the relative distance from the IP (1.4 km, and 1.2 km, respectively), and of the charcoal bags (C1–C8) are displayed.

[63] (Fig. 1). The fault system, both extensional and compressional, are permeability limits, influencing the water level [69] and the groundwater flow direction of the regional aquifer. The aquifer is characterised by a total discharge of about 18–25 m^3/s [63,70] and by net infiltration of 600 mm/y [25]. Campo Imperatore, an endorheic basin in the massif's core, is a preferential recharge area.

This work is focused on two springs located at the north-eastern sector of the aquifer, the Vitella d'Oro and Mortaio d'Angri springs (Fig. 1). These springs, both tapped for drinking purposes, are characterised by mean discharge of 0.6 m^3/s and 0.38 m^3/s, respectively. The Mortaio d'Angri spring is directly fed by the Gran Sasso carbonate aquifer, while the Vitella d'Oro spring is fed also by conglomerate deposits (Rigopiano Conglomerates) [67] (Fig. 2). The impulsive regime of the Vitella d'Oro spring, tapped by an underground drainage tunnel, is associated with the development of the karst network in the Rigopiano Conglomerates.

Therefore, the Mortaio d'Angri spring seems to be directly fed by the regional aquifer, while the Vitella d'Oro spring supply brings together at least three contributions of different origin and characteristics: (i) the base flow, (ii) the direct infiltration into the Rigopiano Conglomerates, and (iii) the karstic network input. This plurality of supply to the Vitella d'Oro spring also determines the occurrence of turbidity phenomena associated with intense and long-lasting meteoric events that cause flow rate increases. The study conducted by Ref. [75] helped define both the hydrogeology and hydrodynamics of the different superficial karst circuits of the Tavo River, also analysing the triggering of the turbidity phenomenon in the Vitella d'Oro spring. By the analysis of almost 500,000 hourly data of turbidity and flow over a period of 26 years, a lack in the biunivocal correspondence between the two values was found; although turbidity is always preceded by a flood, not all increases in flow caused turbidity. Furthermore, it was noticed that solid transport follows floods at Vitella d'Oro spring with a time delay between 0 and 9 h (mode equal to 3 h), recording up to four successive waves of turbidity for a single rainfall event. The turbidity peak usually occurred after 3 h from its initial appearing, and subsequent peaks show a delay between 6 and 11 h (see Figs. S1 and S2 of Supplementary Material). Similar limited correlations have been found between rainfall and turbidity events: the highest number of turbidity events following rainfall occur in October and November, at the end of the exhaustion period. Furthermore, after a high turbidity event, following rainfalls are not capable of triggering new significant turbidity events. The study inferred that turbidity is related to clay levels in Rigopiano Conglomerates, and that these sediments can be remobilized from the karst conduits by the infiltrating water from rainfall or snowmelt.

3. Material and methods

3.1. Hydrogeochemical monitoring

The hydrogeochemical monitoring consists of both discrete and continuous monitoring. In detail, for the continuous monitoring turbidity, temperature, and EC data detected by the field fluorometer at the Vitella d'Oro spring tunneling have been considered. The continuous field fluorometer probe (GGUN FL30), made by Albillia Co. (Neuchatel, Switzerland), hosts different optics for tracer detection, a power supply, and a data logger. The FL30 Albillia probe allows continuous monitoring of up to three different tracers, and, in addition to these, turbidity-independent measurement, EC, and temperature (precision of ±0.1 °C) [30,39,76]. The measuring system consists of four detector sections oriented at an angle of 90°, which contain an almost monochromatic light spring, a filter, and a condensation lens, so the light of a wavelength illuminates the water uniformly [77]. The sampler consists of 4 different lamps: Uranine, Tinopal, Amidorhodamine-G (detection threshold: 0.001 μg/L, 0.1 μg/L, and 0.1 μg/L, respectively), and Turbidity (Turbidity detection: 0.02 to 400 NTU). The greatest advantage of this field device is the rapid access to data (flash memory and/or GPRS transmission) and the complete absence of contamination [77]. The same instrument has been used to investigate the arrival of the two tracers (see paragraph 3.2: "Tracer test set-up and methodology"). The fluorometer in the Vitella D'Oro tunneling has been installed on 28th April 2021. The hydrogeological data have been compared with rainfall data from the Arsita thermopluviometric gauge, the closest one to the monitoring site.

Also, discrete flow rate measurements and hydrogeochemical data have been considered. The daily flow rate data of the Vitella d'Oro and Mortaio d'Angri springs have been obtained from the drinking water supply ACA S. p.A. The Mortaio d'Angri spring is collected both by spring emergency and also by the support of wells, while the Vitella d'Oro spring is collected with a draining tunnel, which pours the overflow of the spring flow, not collected by ACA, into the riverbed of the Tavo River.

Groundwater samples of the Vitella d'Oro and the Mortaio d'Angri springs have been collected to analyse major ions, trace elements, and isotope content. Groundwater samples have been filtered in situ through a 0.45 μm filter and then collected into polyethylene bottles. They have been stored at low temperature to prevent alteration of groundwater composition. Dionex ICS-1100 has been used for analysing cations (Na^+, K^+, Mg^{2+}, Ca^{2+}), whereas Dionex ICS-5000 has been used for anions (F^-, Cl^-, NO_3^-, SO_4^{2-}). Through titration with 0.05 N HCl solution, bicarbonate was determined in the field. Major and trace elements analyses have been carried out at the Geochemical Laboratory, Department of Earth Sciences, Sapienza University of Rome (Italy).

The stable water isotopes (^{18}O and D) contribute to obtaining relevant information on the groundwater origin, the recharge area, and potential mixing processes [78]. They have been collected into polyethylene bottles and stored at low temperatures. The isotope analyses have been performed at IT2E Isotope Tracer Technologies Europe Srl in Milan (Italy). The analytical precision is about ±0.1‰ for $\delta^{18}O$ and ±1‰ for δD [79,80]. Measurements of stable isotopes of water ($\delta^{18}O$ and δD) are expressed in terms of delta units per mil (δ‰). All the geochemical data are available in Table S1 of Supplementary Material.

Based on isotopic data, specific isotopic vertical gradients have been calculated, adopting equations Eq. (1) to assess CIRE (Computed Isotope Recharge Elevation) for Gran Sasso aquifer, [58]:

$$\delta^{18}O = -0{,}0024h - 6.35 \quad (1)$$

where h is the elevation in meters above sea level.

3.2. Tracer test set-up and methodology

The tracer test has been carried out in April 2022 using two of the best-known tracers for this type of technique, namely Uranine (Acid Yellow 73, CAS: 518-47-8, BASF, $C_{20}H_{10}Na_2O_5$, detection threshold: 0.001 μg/L) and Sodium Naphthionate ($C_{10}H_8NNaO_3S$, CAS: 130-13-2, detection threshold: 0.1 μg/L) [10,28,33,44,76,81]. These two tracers are widely used in the field of hydrogeology and are considered toxicologically safe and not impacting on the environment [82]. Uranine has high solubility and its detection limit is very low (~0.005 μg/L) both on the field and in the laboratory [42,82,83]. During the treatment with Uranine, it is relevant to consider its photo-decay. Sodium Naphthionate is a non-adsorbent, safe, and invisible fluorescent dye and has a detection limit of 0.1 μg/L. It can interfere with DOC, not recorded at Vitella d'Oro spring [83,84].

To simulate in advance the tracer test conditions, some 1D scenarios have been assumed considering the result obtained by Ref. [75], which analysed how the turbidity phenomenon is triggered in the Vitella d'Oro spring. In detail, the average shift between discharge rise and turbidity appearance is approximately three and a half hours, ranging from zero 9 h [75]. By this way, 20 g of Uranine, and 100 g of Sodium Naphthionate have been established for the test. In advance, the two dyes have been diluted in the laboratory in a 2-liter solution of water in a sterile container.

The two tracers have been injected inside the Rigopiano ditch (1045 m asl) and have been monitored by the field fluorometer in the downstream area inside the Vitella d'Oro tunnel (FV, 748 m asl), and on the Tavo River upstream of the Vitella d'Oro waterfall (FT, 610 m asl), located just downstream of the confluence of the Rigopiano ditch with the Tavo River. These two monitoring points are 1.2 km and 1.4 km far from the injection point, respectively (Fig. 3).

The injection of the two tracers took place at 1-h intervals. Uranine has been injected into the Rigopiano ditch on 05.04.2022 at 8.15 a.m. and the Naphthionate on 05.04.2022 at 9.15 am.

The acquisition time of the field fluorometers has been set with a frequency of 5 min. In particular, the FV has been installed before the tracer test, in order to monitor possible previous turbidity events. Moreover, traditional sampling has been performed at the two monitoring points. Water samples have been collected in 50 ml amber glass bottles and stored in a box, due to the Uranine photo-decay. In order to record the arrival of the tracer at the monitoring points, traditional sampling started with more frequent sampling intervals at the beginning of the test (every 15 min) and then less frequent intervals (every 1 h) after the estimated time of arrival of peak concentration (approximately 6 h from the start of the test, according to Ref. [75]).

Besides, eight charcoal bags have been installed near the monitoring and injection points. Due to their low cost and their easy application, charcoal bags are commonly used mainly for preliminary tests and out-of-reach sites [42]. The locations of the charcoal bags are illustrated in Fig. 3. After the end of the test, the charcoal bags have been taken and then replaced with new ones at the same locations in case the tracer could arrive even after the end of the test.

Once the tracer test has been completed, water samples collected during the tracer test and the charcoal bags have been analysed

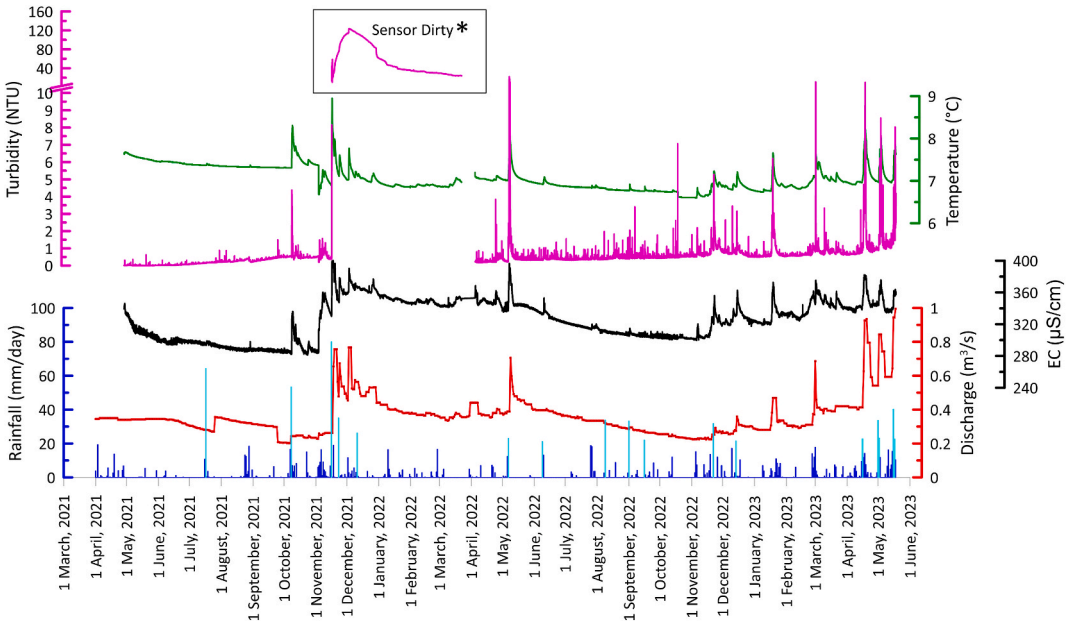

Fig. 4. Time series of rainfall, turbidity, temperature, EC, and flow rate from 28.04.2021 to 06.04.2023. Rainfall (mm/day) is displayed with blue bars and rainfall events that exceed 20 mm/day are depicted with light blue bars. Turbidity (NTU), temperature (°C), EC (μS/cm), and discharge (m^3/s) are shown with reddish purple, green, black, and red lines, respectively. Data anomaly of turbidity due to sensor disabled by the coating is displayed by (*).

using the Perkin Elmer LS 55 laboratory fluorometer (or fluorescence spectrometer) in the laboratory of the University of Karlsruhe Institute of Technology (KIT) in Germany.

Each fluorescent dye has specific spectra characteristics, such as absorption maxima, fluorescence maxima, wavelength, and relative fluorescence efficiency. The occurrence of the fluorescent dye in the sample is pointed out by the presence of the associated peak in the sample spectrum. Considering the two tracers used, Uranine and Naphthionate, absorption maxima are at 490 nm and 320 nm, respectively [85].

The laboratory fluorometer is connected to the computer and the results are visible through the BL Studio software. Before analysing the samples, the instrument has been calibrated using previously prepared standards for both Uranine and Naphthionate.

4. Results and discussion

4.1. Hydrogeological and hydrogeochemical findings

Prior to the tracer test, data obtained from hydrogeological monitoring since April 2021 to May 2023 have been analysed. The Fig. 4 show the time series of rainfall, discharge, EC, turbidity, and temperature. In particular, rainfall data are characterised by a maximum value of 80 mm/day recorded on 16th October 2021 and the average amount of rain during the monitoring period is 866 mm/y. The maximum discharge value is equal to 0.99 m^3/s, and the minimum value is 0.2 m^3/s, with an average value of 0.36 m^3/s. The EC is defined by a maximum value of 400 μS/cm, a minimum value of 278 μS/cm, and a mean value of 324 μS/cm. Concerning turbidity, the maximum value is 21.9 NTU, and the minimum value is 0 NTU with an average value of 0.51 NTU. Temperature has a maximum value of 8.9 °C, a minimum value of 6.6 °C, and an average value of 7 °C.

Analysing data recorded by the field fluorometer, together with rainfall and flow rate data, a direct correlation among signals can be observed. Increases in discharge, EC, temperature, and turbidity have been observed after rainfall that exceeds 20 mm/day. Rainfall events exceeding 20 mm/day and the related changes of the studied parameters are shown in Table 1. However, some changes in the considered parameters did not occur in conjunction with intense rainfall events (i.e., >20 mm/day), but they can be associated with consecutive rainy days (for example January 2023 and February 2023). Between November 2021 and April 2022, a data gap of turbidity has been identified due to the sensor damage.

The hydrochemistry of the Vitella d'Oro and Mortaio d'Angri springs is essentially characterised by the abundance of Calcium and Magnesium, with extremely low values of Sodium and Potassium (see data in Table S1 of Supplementary Material). In particular, according to the average values of the ion concentrations (expressed in meq/L), the water of the two springs can be attributed to the bicarbonate-calcium hydrochemical facies, as can be seen in the Schoeller Diagram in Fig. 5a.

The major ion content is lower at Vitella d'Oro and higher at Mortaio d'Angri, with congruent difference confirming a common origin of groundwater flow. Nevertheless, Vitella d'Oro spring shows a significantly higher concentration of sulphates than Mortaio d'Angri spring in all samples. This anomaly indicates a different flowpath, which would have origin in the Rigopiano Conglomerates aquifer. These additional sulphates contribution is coming from the interaction with gypsum coming Messinian evaporitic levels and/or migrated in fractures of the recent extensional tectonic phase [51,61]. In particular, the major increases in the concentration value of SO_4 have been recorded in March 2021 (36 mg/L) and in May 2022 (21 mg/L), in correspondence with the snow melting period, when additional infiltration through the Conglomerates aquifer is able to mobilize high content in sulphates. In Table 2 the concentrations of sulphates in Vitella d'Oro and Mortaio d'Angri springs are reported.

Based on stable isotope values during the period 2020–2022 (Fig. 5b and data in Table 3), the CIRE calculation (Fig. 5c and Table 3) have been obtained by 58. They predict an average recharge elevation of the Vitella d'Oro spring of 1676 m asl., and a slightly higher for Mortaio d'Angri spring at 1768 m asl. The springs show stable values of $\delta^{18}O$ (average: 10.5‰) and are characterised by a CIRE between 1600 m asl and 1800 m asl, which can be correlated with the altitudes of the Campo Imperatore endorheic basin. Therefore, it

Table 1
Rainfall events that exceed 20 mm/day are reported. Also, increase of discharge, EC, temperature and turbidity with respect to the previous data are shown.

ID	Date	Rainfall (mm/day)	Discharge Change [m^3/s]	EC Change [μS/cm]	Temperature Change [°C]	Turbidity Change [NTU]
1	17/07/2021	64.2	+0.1			
2	08/10/2021	53.4	+0.04	+55	+1	+2.9
3	16/11/2021	80	+0.5	+121	+2.1	+7.8
4	23/11/2021	35	+0.2	+34	+0.5	
5	11/12/2021	26.2	+0.3	+135	+0.1	
6	07/05/2022	23	+0.3	+52	+1	+20.9
7	09/06/2022	21.2		+4	+0.1	
8	09/08/2022	33.8				
9	01/09/2022	33.2			+0.2	+1.7
10	16/09/2022	22			+0.1	+1
11	22/11/2022	31.8	+0.1	+33	+0.4	+4.4
12	14/12/2022	21.4	+0.1	+17	+0.2	+2.1
13	16/04/2023	22.8	+0.5	+291	+0.4	+2.4
14	01/05/2023	33.6	+0.3	+13	+0.2	+1
15	16/05/2023	40.2	+0.4	+405	+0.7	+3.2

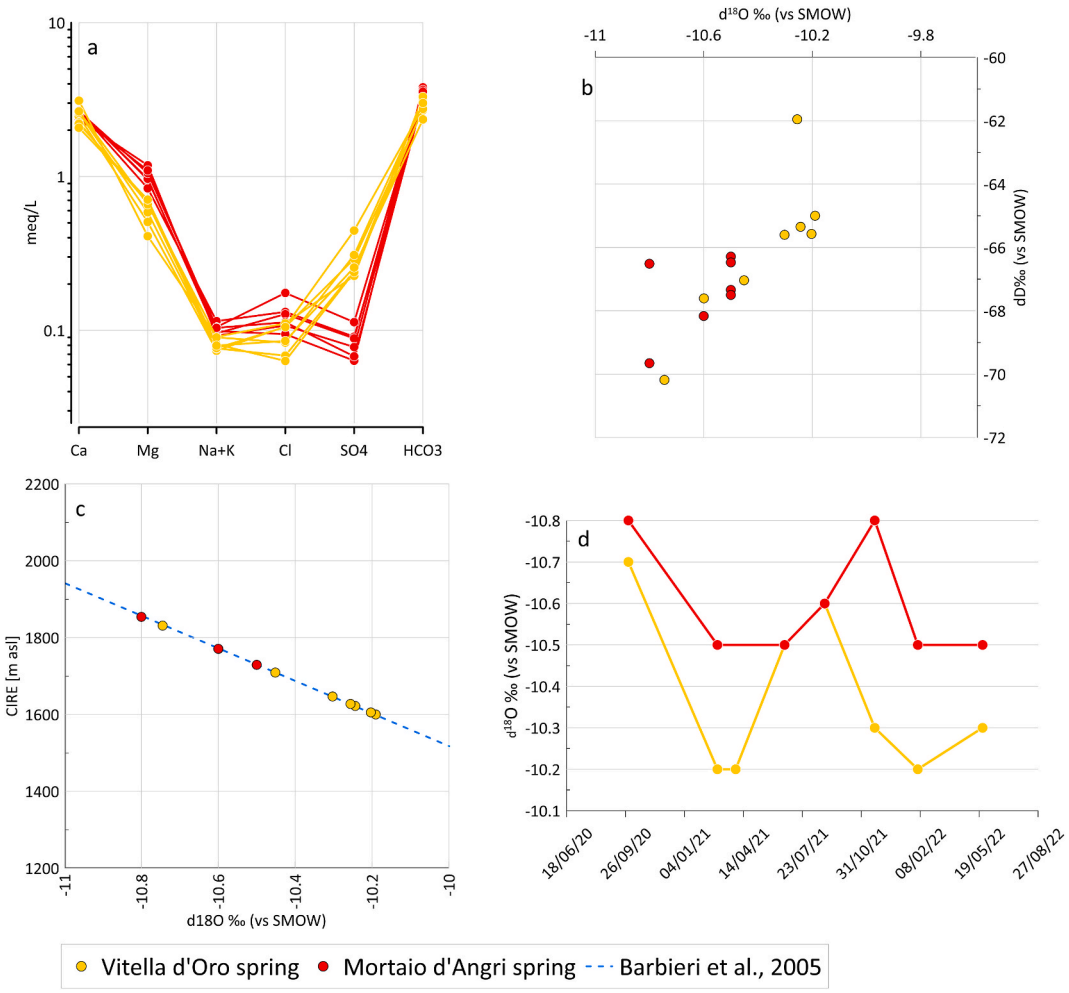

Fig. 5. a) Schoeller diagram; b) Correlation between $\delta^{18}O$ and $\delta^{2}H$ values; c) Correlation line between $\delta^{18}O$ and altitude (CIRE from 58); d) Trends of $\delta^{18}O$ of the two springs during 2020–2022. Vitella d'Oro spring is displayed with yellow colour and Mortaio d'Angri spring is depicted with red colour.

Table 2
Concentration of sulphates (mg/L) measured at Vitella d'Oro and Mortaio d'Angri springs during the hydrogeochemical monitoring. n.a.: not available.

Date	SO_4^{2-} [mg/L]	
	Vitella d'Oro spring	Mortaio d'Angri spring
27/10/2020	12.3	3.3
01/03/2021	36.0	5.6
28/04/2021	14.8	n.a.
23/06/2021	11.5	3.7
30/08/2021	14.0	5.4
23/11/2021	10.9	4.3
04/02/2022	11.7	3.1
25/05/2022	21.4	4.4

can be assumed that the Campo Imperatore basin contributes significantly to the recharge of both springs [80]. Besides, CIRE values of the Vitella d'Oro spring are on average lower than those of the Mortaio d'Angri spring, and values match only in a few cases/periods (Fig. 5c).

This isotopic difference between the two springs corroborates the conceptual model of a recharge area only partially overlapping. In fact, the lower CIRE for Vitella d'Oro is congruent with a contribution from the Conglomerates aquifer, outcropping a lower elevation (see Fig. 2). At the same time, isotopic values of Mortaio d'Angri are steady, as expected from a regional recharge area

Table 3
Stable isotopes (δ^2H, $\delta^{18}O$) and CIRE values of the period 2020–2022 (obtained by 58).

Vitella d'Oro spring	Date	δ^2H	$\delta^{18}O$	CIRE (m asl)
	01/10/2020	−70.2	−10.7	1792
	01/03/2021	−65.3	−10.2	1608
	01/04/2021	−65.0	−10.2	1608
	23/06/2021	−67.0	−10.5	1725
	30/08/2021	−67.6	−10.6	1776
	23/11/2021	−62.0	−10.3	1626
	04/02/2022	−65.6	−10.2	1608
	25/05/2022	−65.6	−10.3	1626
Mortaio d'Angri spring	**Date**	**δ^2H**	**$\delta^{18}O$**	**CIRE**
	01/10/2020	−69.7	−10.8	1850
	01/03/2021	−67.3	−10.5	1725
	23/06/2021	−67.5	−10.5	1725
	30/08/2021	−68.2	−10.6	1776
	23/11/2021	−66.5	−10.8	1850
	04/02/2022	−66.3	−10.5	1725
	25/05/2022	−66.5	−10.5	1725

(Campo Imperatore and the main Gran Sasso aquifer), while slight but significant differences have been recorded for Vitella d'Oro stable isotopes. Coherently with the conceptual model obtained by hydrochemical content, it has been noted that during depletion period (e.g. summer dry semester) the isotopic values of the two springs are very similar and frequently coincide (see Fig. 5d), while during recharge period (e.g. winter rainy/snowy semester) a lowering of CIRE in Vitella d'Oro clearly expresses the local infiltration, which becomes prevalent during intense meteoric events and snowmelt occurrence. Similar observations descend from the statistical analysis of discharge data. In detail, recharge (Fig. 6a and b) and depletion period (Fig. 6c and d) has been investigated for the last two years. Fig. 6 shows similar discharge and dispersion in the depletion period for the two springs. Nevertheless, during the recharge period, Vitella d'Oro spring values are not only higher than in Mortaio d'Angri, but the discharge shows a greater variability and

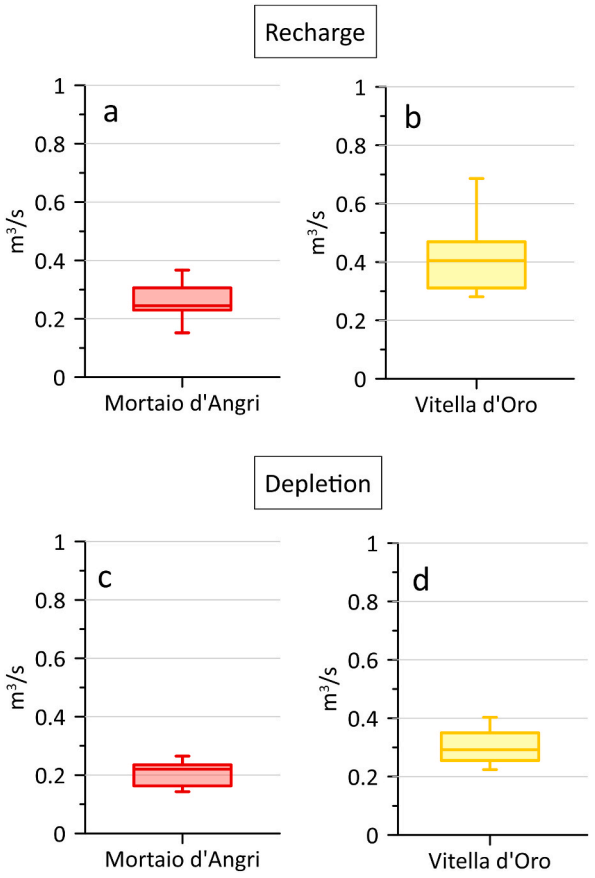

Fig. 6. Box and whiskers plots analysis for Mortaio d'Angri (in red) and Vitella d'Oro (in yellow) springs for 2020–2022 period. Recharge period is displayed in boxes a and b, while depletion period is shown in boxes c and d.

frequent peaks (Fig. 6b), attributable to the contribution coming from the Rigopiano Conglomerates.

The Tritium isotope data helped to shed light on the above-mentioned different origin and also on the relative ages of groundwater. Tritium values (expressed in Tritium Unit, TU), collected since March 2021 to February 2022, are shown in Table 4. Samples of Vitella d'Oro spring are characterised by tritium values of about 4 TU that are correlated with possible faster-flowing groundwater flowpaths. However, in karst context, mean tritium values can be up to 16 TU [86–88]. In this framework, the fast flow of the Vitella d'Oro spring through the Rigopiano Conglomerates has a karstic component whose contribution to the spring discharge is not negligible. On the other hand, tritium values for Mortaio d'Angri spring are close to 2 TU, indicating longer residence times related to the regional basal flow.

In fact, additional monitored data (i.e., EC and turbidity but also discharge peaks), confirm the arrival at the Vitella d'Oro tunneling of recharge correlated with intense meteoric events (see Fig. 4 and Table 1). All these information confirms the complex flowpath and the different origin of recharge at Vitella d'Oro spring, requiring additional investigations.

4.2. Tracer test findings

Through the analysis of the samples at the monitoring point of the Vitella d'Oro (FV) tunneling, the arrival of both tracers has been observed 11 h after the tracer injection. In particular, the maximum peak of Uranine has been recorded at 00:00 on 06.04.2022 (0.052 μg/L), while the maximum peak of Naphtionate has been recorded at 02:00 on 06.04.2022 (0.35 μg/L).

In the Tavo River, upstream of the Vitella d'Oro (FT) overflow by waterfall, the arrival of the two tracers has been observed 9 h and 45 min after the tracer injection. The maximum peak has been recorded at 20:00 for Uranine (0.15 μg/L) and 21:00 for Naphthionate (0.85 μg/L).

The results from the water samples show firstly the arrival of the tracers in the FT and subsequently at the FV, differently to what was expected, based on the distance between the monitoring points and injection point. The difference in the arrival time of the tracers at the two monitoring points is approximately 1 h and 15 min.

Subsequently, data acquired by the Fluorometer Albillia FL30 have been also analysed, particularly for Uranine, because the fluorometer was unable to detect Naphthionate. The background noise recorded by the fluorometer has been filtered. Then, comparing the correct data to the analysis of water samples, a congruence of the Uranine results between the two methods has been observed. In fact, the time of tracer arrival and the time of peak maximum match. The differences in peak concentrations depend mainly on the calibration of the field fluorometer, which is not in perfect agreement with the laboratory fluorometer (Fig. 7).

The tracing technique leads to the generation of a tracer breakthrough curve (BTC), which provides considerable information on the aquifer, groundwater flow, contaminant transport, and conduit network [44].

At FV, the tracer recovery has been calculated to be approximately 6.1% for Uranine and 4.9% for Naphthionate. At FT, the recovery has been observed for Uranine and Naphthionate of 14.3% and 12.3%, respectively (Fig. 8). The low recovery percentage could be because of a part of the water could go elsewhere, to remote or deeper springs that cannot be monitored, or due to the non-ideal injection conditions (e.g. decay in the sunlight, when the tracer was injected during daytime in a surface stream; or adsorption on rock surfaces). However, the two BTC are very similar, testifying the reliability of the test. In addition, the results confirmed the different recharge area feeding the Vitella d'Oro spring, characterised by the presence of the karst network of Rigopiano recharge area.

To further verify the BTC, the STANMOD software has been used with the code CXTFIT [89]. This approach allows to quantify the parameters of the transport model. The program can also be used to determine the concentration as a function of time and/or space, and to estimate pore water velocity and the dispersion coefficient. In the case study, a two-region non-equilibrium (2RNE) model of CXTFIT has been adopted [89]. 2RNE has been used to calibrate the initial estimates of the solute transport parameters starting from the BTC tracer curves developed from site tests.

The R^2 value, obtained from the 2RNE model, varies between 0.95 and 0.98, showing a high correlation between the real and theoretical series of data. The pore water velocity values and the dispersion coefficients are reported in Table 5.

As already mentioned, in addition to the use of the field fluorometer and the analysis of water samples collected during the tracer test, 16 charcoal bags have been installed, in 8 sites, during the test and immediately afterward. By examining the activated charcoal bags, Uranine has been detected in 6 out of 8 monitoring points (C2–C4, C6–C8) (Fig. 3). The tracer has been also identified in the charcoal bags installed after the test. This result is a clear sign of the presence of slower groundwater flowpaths with different response times. At the remaining two monitoring points (C1, C5), however, no tracer has been detected either during or after the test (Fig. 3). The two charcoal bags in which Uranine has not been observed are located at the Mortaio d'Angri spring and in a little spring in the Vitella d'Oro tunnel, out of the main drainage system. In Table 6 the detected concentration of the Uranine inside the charcoal bag is shown.

Therefore, the tracer test confirmed the role of Rigopiano ditch in recharging the local aquifer, but it reaches the Vitella d'Oro

Table 4
Tritium data of Vitella d'Oro and Mortaio d'Angri springs.

	^{3}H (TU) Vitella d'Oro spring	^{3}H (TU) Mortaio d'Angri spring
01/03/2021	4.1	2.2
23/06/2021	4.1	2.2
30/08/2021	3.7	1.7
04/02/2022	4.6	2.1

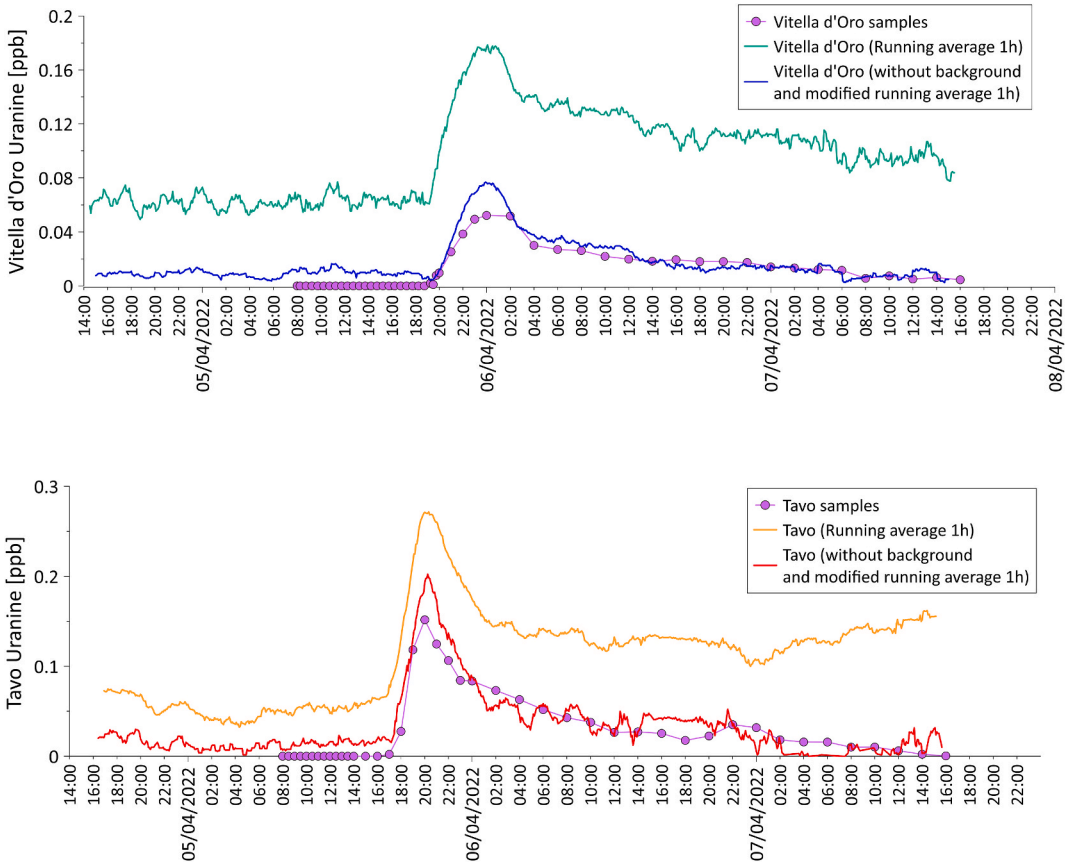

Fig. 7. Comparison between data from the field fluorometer and data of samples analysed in the laboratory. In light blue and orange, the field fluorometer data with background noise. In dark blue and in red the field fluorometer data without background noise. In purple the data obtained by the analyses of samples.

spring with reduced percentages, leading to two different conclusions: the discharge of the spring is limitedly but significantly fed by a karstic component of fast flow; secondly, the karst network is not releasing immediately the local input, having additional components with longer response times. In fact, during the 48 h following the arrival of the tracer, the additional recovery has been calculated just over 20% of the tracer. This evidence confirms the existence of a deeper and more complex flow into the Conglomerates aquifer by karst network, with longer response times, but able to feed both the Vitella d'Oro spring and Tavo River, as stated by the tracer found in the charcoal bags in the post-test period.

To sum up, the tracer test can be successfully evaluated, confirming and detailing the complex dynamic of recharge and groundwater flow at Vitella d'Oro spring respect with the twin spring of Mortaio d'Angri. In detail, three different components of the spring discharge can be distinguished, as follows.

The base flow of Vitella d'Oro discharge is fed by the Gran Sasso regional aquifer, having a common origin with Mortaio d'Angri spring, as shown by hydrochemical analyses; this base flow ensures the minimum discharge of the spring and it is regulated by the regional recharge (especially in Campo Imperatore); it is still unclear how the groundwater overpasses the hydraulic limit of the westernmost regional thrust, but the recent extensional tectonic, locally intercepting the thrust, and the presence of the Calcarenitic local aquifer are sufficient to host groundwater resources between the two thrusts.

The role of the locally karstified Rigopiano Conglomerates offers additional components to the recharge feeding only Vitella d'Oro spring; the tracer test results, but also the hydrochemical and isotopic data shed light on the additional contribution and the discharge changes at the spring; in fact, it is unusual to have such high variability of spring discharge in a tunnel drainage, which represents a fixed level of drainage for groundwater [90–92].

The karst contribution by Conglomerates shows two different components: a fast one is clearly evidenced by the tracer test results. In absence of surface karst landforms, the recharge is driven by the ditches, with fast infiltration into the underground karst system; the transfer towards the destination points (e.g., the tunnel drainage of Vitella d'Oro, but also the Tavo River as local base level of groundwater flow) is fast (about 35 m/h for Vitella d'Oro spring and 65 m/h for Tavo River) but not immediate.

This condition, also testified by a rise in EC (which usually is expected to decrease during the recharge period), is clearly occurring during extreme events of rainfall, but the major turbidity is recorded in coincidence with the big rainfall event at the end of the summer season, not necessarily replicated by the following ones during the recharge season, in accordance with previous results [75].

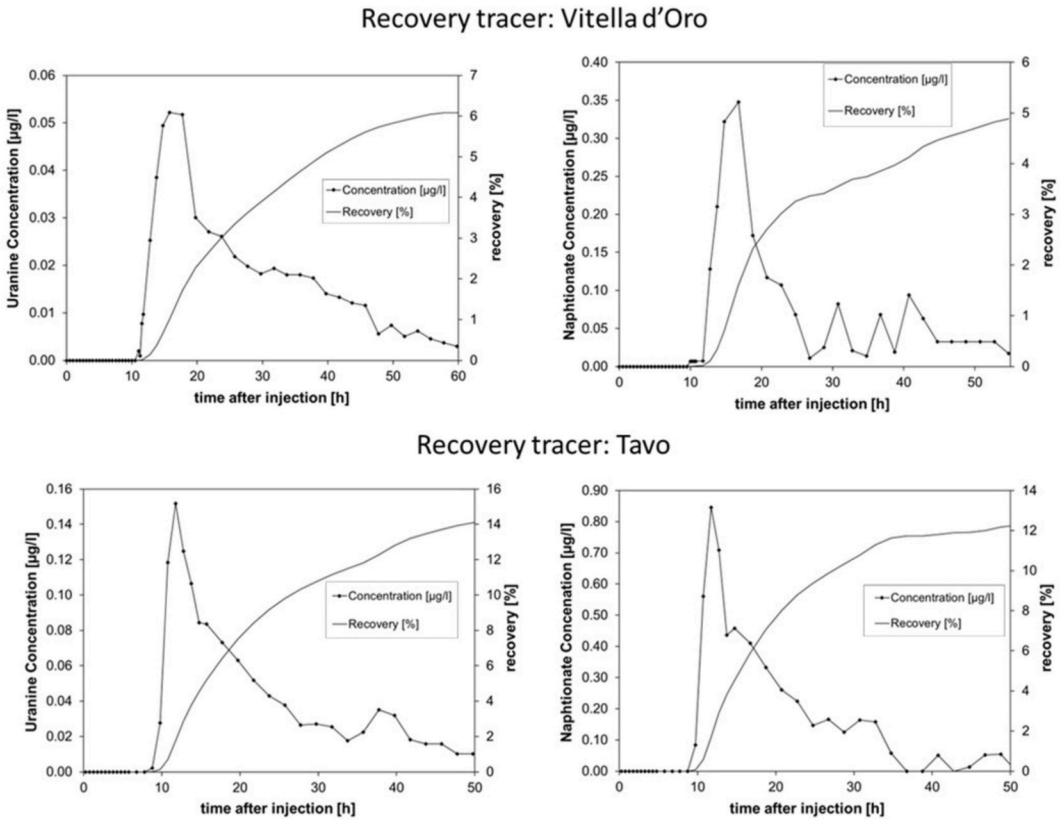

Fig. 8. BTC results of the two tracer in the two monitoring points (on top BTC of Uranine (left) and Naphtionate (right) concentration at the Vitella d'Oro tunneling (FV); on bottom: BTC of Uranine (left) and Naphtionate (right) concentration at the Tavo River (FT).

Table 5
Data of pore water velocity values V(m/h) and the dispersion coefficients D (m^2/h) calculated for FV and FT monitoring points.

	V(m/h)		D (m^2/h)	
	FV	FT	FV	FT
U	37	61	498	441
Na	30	70	339	332

Table 6
Concentration of the Uranine detected in the charcoal bags. +++: high concentration, ++: medium concentration, +: low concentration.The ID of the charcoals are followed by "_1" and "_2" which indicate the first installed charcoal bags and the second ones, respectively.

ID	Concentration	ID	Concentration
C1_1	NO TRACER	**C6_1**	++
C1_2	NO TRACER	**C6_2**	+
C2_1	+++	**C7_1**	+
C2_2	+++	**C7_2**	+
C3_1	+	**C8_1**	+
C3_2	+	**C8_2**	+
C4_1	+		
C4_2	+		
C5_1	NO TRACER		
C5_2	NO TRACER		

A second component of infiltration by the karst system is subjected to a slower release into the spring discharge, as testified by the charcoal bags collecting the tracer in the following week respect with the tracer test. Thus, the karst network continues to feed the Vitella d'Oro tunnel drainage, representing the longer-flow component correlated to the Conglomerates aquifer, as testified by the high

content in sulphates respect with the regional groundwater flow recorded at Mortaio d'Angri. It is supposed that this component is gradually lowering with time, until a new rainfall event is able to push towards the spring the sediment trapped in the karst system; a final confirmation of this conceptual model comes from the Tritium isotope, which differently from Mortaio d'Angri spring, evidences clear recent contribution in Vitella d'Oro discharge (see Table 4).

5. Conclusion

The management of groundwater resource requires optimization to successfully tackle the challenges raised by the occurrence of extreme events (both droughts and high-rate rainfall), having clear effects on aquifer recharge and consequently competing with the need to guarantee a regular drinking water supply. It is well known that karst aquifers constitute a priorital source of drinking water, especially in Mediterranean area, where coastal and alluvial aquifers are often menaced by direct human pressures. The availability of high-quality groundwater coming from mountainous regions, frequently corresponding to environmental protected areas, is fundamental, and karst aquifers can host huge amounts of groundwater resources due to their high permeability; of course, their vulnerability directly depends on the evolution of the karst system, reflecting not only in water quality but also in irregular discharge rate.

In this framework, the Gran Sasso aquifer shows all the characteristics needed for satisfying water demand but also preserving environmental values and related ecosystem services. The two tapped springs of the high Tavo River Valley have a common origin and general hydrochemical content, but they clearly distinguish for their regime and response to recharge input. These differences are due to the karst behaviour, and the overlapping of a local karstified aquifer (Rigopiano Conglomerates) on the regional fractured aquifer.

For Vitella d'Oro spring, the presence of karstic networks determines a rapid response to meteoric events, making the spring particularly sensitive to both basin-scale variations and extremely local recharge conditions, in terms of discharge variability and of turbidity content, which would be correlated to potential pollution events if any. By the execution of a tracer test, a very detailed conceptual model has been developed, evidencing a triple source of recharge of the spring:

i) the base flow, similar to Mortaio d'Angri spring, fed by recharge of the regional aquifer, which guarantees the minimum flow of about 150 L/s also during exhaustion periods;
ii) a fast flow directly related to rainfall and snowmelt events in the local aquifer, which has been characterised by the tracer test in terms of recovery rate and dispersivity (reported in Table 4); this is responsible for discharge peaks coupled with relevant turbidity content, revealing the presence of karst conduits;
iii) a non-fast karst flow, which is released into the Vitella d'Oro tunnel drainage system with time respect to the rainfall events, and which sustains the spring discharge with very limited content or absence of turbidity, ensuring a higher tapped discharge at the beginning of the exhaustion phase.

This detailed conceptual model is based on general hydrogeological conditions, but it has been validated by the use of hydrochemical and isotope information, able to distinguish between the two spring regimens, opening the door for a water management optimization, offering the possibility to separate the resource availability of both springs. The tracer test confirms to be a valuable tool for detailing and quantifying the groundwater flow in karst systems, also with limited evolution in term of karst conduits.

Thus, the main findings of the study can be considered useful both: i) from the methodological point of view, where tracer tests confirmed to be a fundamental tool to shed light on detailed groundwater flow, and ii) from the management one, offering the future possibility to the drinking water supplier for a diversification of its withdrawals on the basis of natural availability in wet, normal and drought conditions, taking into account the different vulnerability of the two springs.

In detail, Vitella d'Oro tunnel drainage has been defined to be subjected to variable vulnerability conditions, with changes during different discharge phases. The vulnerability to pollution is high during rainfall and snowmelt period (towards very high in correspondence with first Fall significant events), becoming medium to low during the exhaustion phase, when the recharge contribution from the Conglomerates aquifer is lowering, until disappearing in drought conditions.

Finally, it can be stated that: i) clear advancement on the knowledge on the functioning of limited karstified aquifers can be validated by tracer tests, having direct applications on water resources management, and ii) the transferability of this knowledge to the stakeholders must be included in the mission of hydrogeologists to "make the invisible visible".

Funding

The research has been supported by the European Commission through the Partnership for Research and Innovation in the Mediterranean Area (PRIMA) programme under Horizon 2020 (KARMA project, grant agreement number 01DH19022A).

CRediT authorship contribution statement

V. Lorenzi: Writing - review & editing, Writing - original draft, Visualization, Validation, Software, Methodology, Investigation, Formal analysis, Data curation, Conceptualization. **F. Banzato:** Methodology, Investigation, Conceptualization. **M.D. Barberio:** Writing - review & editing, Writing - original draft, Visualization, Validation, Software, Methodology, Investigation, Formal analysis, Data curation, Conceptualization. **N. Goeppert:** Writing - original draft, Investigation, Data curation. **N. Goldscheider:** Writing - review & editing, Writing - original draft, Supervision, Methodology, Formal analysis, Data curation. **F. Gori:** Writing - review & editing, Writing - original draft, Visualization, Validation, Methodology, Investigation, Formal analysis, Data curation,

Conceptualization. **A. Lacchini:** Methodology, Investigation. **M. Manetta:** Methodology, Investigation. **G. Medici:** Writing - original draft, Validation. **S. Rusi:** Writing - original draft, Validation, Supervision. **M. Petitta:** Writing - review & editing, Writing - original draft, Validation, Supervision, Project administration, Methodology, Funding acquisition, Formal analysis, Conceptualization.

Declaration of competing interest

The authors declare the following financial interests/personal relationships which may be considered as potential competing interests:

Marco Petitta reports financial support was provided by Partnership for Research and Innovation in the Mediterranean Area Italy (KARMA project, grant agreement number 01DH19022A) Horizon 2020, European Union. If there are other authors, they declare that they have no known competing financial interests or personal relationships that could have appeared to influence the work reported in this paper.

Acknowledgments

Authors would like to thank the A.C.A. S. p.A water supply and Regional Environmental Agency (ARTA Abruzzo), for supplying discharge data. Thanks go to IT2E Isotope Tracer Technologies Europe Srl. (Milan, Italy) for the analyses of the isotopic content. Moreover, all members of the Quantitative Hydrogeology Lab, Earth Sciences Department, Sapienza University of Rome are thanked for their logistic and technical support. Discussions with the KARMA project partners during remote meetings, and consequent suggestions, were also highly appreciated. We thank the four anonymous reviewers for their useful criticism, which allow to build a significantly improved manuscript.

Appendix A. Supplementary data

Supplementary data to this article can be found online at https://doi.org/10.1016/j.heliyon.2024.e24663.

References

[1] D.C. Ford, P. Williams, Karst Hydrogeology and Geomorphology, Wiley, Chichester, 2007, p. 562, https://doi.org/10.1002/9781118684986.
[2] A. Hartmann, M. Mudarra, B. Andreo, A. Marín, T. Wagener, J. Lange, Modeling spatiotemporal impacts of hydroclimatic extremes on groundwater recharge at a Mediterranean karst aquifer, Water Resour. Res. 50 (2014) 6507–6521, https://doi.org/10.1002/2014WR015685.
[3] Z. Chen, Modeling a Geologically Complex Karst Aquifer System, Hochifen-Gottesacker, Alps, Doctoral Dissertation, Dissertation, Karlsruhe, Karlsruher Institut für Technologie (KIT), 2017.
[4] Z. Stevanović, Karst waters in potable water supply: a global scale overview, Environ. Earth Sci. 78 (23) (2019) 662, https://doi.org/10.1007/s12665-019-8670-9.
[5] N. Goldscheider, Z. Chen, S.A. Auler, M. Bakalowicz, S. Broda, D. Drew, J. Hartmann, G. Jiang, N. Moosdorf, Z. Stevanovic, G. Veni, Global distribution of carbonate rocks and karst water resources, Hydrogeol. J. 28 (2020) 1661–1677, https://doi.org/10.1007/s10040-020-02139-5.
[6] J. Xanke, N. Goldscheider, M. Bakalowicz, J.A. Barberá, S. Broda, Z. Chen, M. Ghanmi, A. Günther, A. Hartmann, H. Jourde, T. Liesch, M. Mudarra, M. Petitta, N. Ravbar, Z. Stevanovic, Mediterranean Karst Aquifer Map (MEDKAM), 1:5,000,000, 2022, https://doi.org/10.25928/MEDKAM.1. Berlin, Karlsruhe, Paris.
[7] W.B. White, A brief history of karst hydrogeology: contributions of the NSS, J. Cave Karst Stud. 69 (1) (2007) 13–26.
[8] A. Hartmann, T. Wagener, A. Rimmer, J. Lange, H. Brielmann, M. Weiler, Testing the realism of model structures to identify karst system processes using water quality and quantity signatures, Water Resour. Res. 49 (6) (2013) 3345–3358, https://doi.org/10.1002/wrcr.20229.
[9] Z. Chen, A. Hartmann, T. Wagener, N. Goldscheider, Dynamics of water fluxes and storages in an Alpine karst catchment under current and potential future climate conditions, Hydrol. Earth Syst. Sci. 22 (7) (2018) 3807–3823, https://doi.org/10.5194/hess-22-3807-2018.
[10] N. Goldscheider, D. Drew, Methods in Karst Hydrogeology, International Contribution to Hydrogeology, IAH, Taylor and Francis/Balkema, London, 2007, p. 26.
[11] L. Kiraly, Karstification and groundwater flow, in: Proceedings of the Conference on Evolution of Karst: from Prekarst to Cessation, 2002, pp. 155–190. Postojna-Ljubljana.
[12] D.J. Vesper, W.B. White, Metal transport to karst springs during storm flow: an example from Fort Campbell, Kentucky/Tennessee, USA, J. Hydrol. 276 (1–4) (2003) 20–36, https://doi.org/10.1016/S0022-1694(03)00023-4.
[13] Z. Chen, N. Goldscheider, Modeling spatially and temporally varied hydraulic behavior of a folded karst system with dominant conduit drainage at catchment scale, Hochifen–Gottesacker, Alps, J. Hydrol. 514 (2014) 41–52, https://doi.org/10.1016/j.jhydrol.2014.04.005.
[14] L. Király, G. Morel, Remarques sur l'hydrogramme des sources karstiques simulé par modèles mathématiques: avec 15 figures, Bull. Cent. Hydrogeol. 1 (1976) 37–60.
[15] A. Kovács, Estimation of conduit network geometry of a karst aquifer by the means of groundwater flow modeling (Bure, Switzerland), Bol. Geol. Min. 114 (2) (2003) 183–192.
[16] R. Stephen, H. Worthington, Diagnostic hydrogeologic characteristics of a karst aquifer (Kentucky, USA), Hydrogeol. J. 17 (7) (2009) 1665, https://doi.org/10.1007/s10040-009-0489-0.
[17] M. Bakalowicz, Karst groundwater: a challenge for new resources, Hydrogeol. J. 13 (2005) 148–160, https://doi.org/10.1007/s10040-004-0402-9.
[18] W.E. Winston, R.E. Criss, Dynamic hydrologic and geochemical response in a perennial karst spring, Water Resour. Res. 40 (5) (2004).
[19] B. Trček, Flow and solute transport monitoring in the karst aquifer in SW Slovenia, Environ. Geol. 55 (2008) 269–276, https://doi.org/10.1007/s00254-007-1001-6.
[20] N. Ravbar, J.A. Barberá, M. Petrič, J. Kogovšek, B. Andreo, The study of hydrodynamic behaviour of a complex karst system under low-flow conditions using natural and artificial tracers (the catchment of the Unica River, SW Slovenia), Environ. Earth Sci. 65 (2012) 2259–2272, https://doi.org/10.1007/s12665-012-1523-4.
[21] N. Ravbar, M. Petrič, M. Blatnik, A. Švara, A multi-methodological approach to create improved indicators for the adequate karst water source protection, Ecol. Indicat. 126 (2021) 107693, https://doi.org/10.1016/j.ecolind.2021.107693.
[22] A.I. Marín, B. Andreo, M. Mudarra, Vulnerability mapping and protection zoning of karst springs. Validation by multitracer tests, Sci. Total Environ. 532 (2015) 435–446, https://doi.org/10.1016/j.scitotenv.2015.05.029.

[23] N. Goepper, N. Goldscheider, Improved understanding of particle transport in karst groundwater using natural sediments as tracers, Water Res. 166 (2019) 115045, https://doi.org/10.1016/j.watres.2019.115045.
[24] C. Ollivier, N. Mazzilli, A. Olioso, K. Chalikakis, S.D. Carrière, C. Danquigny, C. Emblanch, Karst recharge-discharge semi distributed model to assess spatial variability of flows, Sci. Total Environ. 703 (2020) 134368, https://doi.org/10.1016/j.scitotenv.2019.134368.
[25] V. Lorenzi, C. Sbarbati, F. Banzato, A. Lacchini, M. Petitta, Recharge assessment of the Gran Sasso aquifer (Central Italy): time-variable infiltration and influence of snow cover extension, J. Hydrol. Reg. Stud. 41 (2022) 101090, https://doi.org/10.1016/j.ejrh.2022.101090.
[26] V. Živanović, Delineation of Karst Groundwater Protection Zones, Karst Aquifers—Characterization and Engineering, Springer International Publishing, Switzerland, 2015, pp. 625–642.
[27] P. Turpaud, L. Zini, N. Ravbar, F. Cucchi, M. Petrič, J. Urbanc, Development of a protocol for the karst water source protection zoning: application to the Classical Karst Region (NE Italy and SW Slovenia), Water Resour. Manag. 32 (2018) 1953–1968, https://doi.org/10.1007/s11269-017-1882-4.
[28] U. Lauber, N. Goldscheider, Use of artificial and natural tracers to assess groundwater transit-time distribution and flow systems in a high-alpine karst system (Wetterstein Mountains, Germany), Hydrogeol. J. 22 (8) (2014) 1807.
[29] L. Dewaide, I. Bonniver, G. Rochez, V. Hallet, Solute transport in heterogeneous karst systems: dimensioning and estimation of the transport parameters via multi-sampling tracer-tests modelling using the OTIS (One-dimensional Transport with Inflow and Storage) program, J. Hydrol. 534 (2016) 567–578, https://doi.org/10.1016/j.jhydrol.2016.01.049.
[30] J.A. Barberá, M. Mudarra, B. Andreo, B. De la Torre, Regional-scale analysis of karst underground flow deduced from tracing experiments: examples from carbonate aquifers in Malaga province, southern Spain, Hydrogeol. J. 26 (1) (2018) 23–40, https://doi.org/10.1007/s10040-017-1638-5.
[31] R. Benischke, Advances in the methodology and application of tracing in karst aquifers, Hydrogeol. J. 29 (1) (2021), https://doi.org/10.1007/s10040-020-02278-9.
[32] N. Goldscheider, Karst groundwater vulnerability mapping: application of a new method in the Swabian Alb, Germany, Hydrogeol. J. 13 (2005) 555–564, https://doi.org/10.1007/s10040-003-0291-3.
[33] M. Mudarra, B. Andreo, A.I. Marín, I. Vadillo, J.A. Barberá, Combined use of natural and artificial tracers to determine the hydrogeological functioning of a karst aquifer: the Villanueva del Rosario system (Andalusia, southern Spain), Hydrogeol. J. 22 (5) (2014) 1027, https://doi.org/10.1007/s10040-014-1117-1.
[34] A. Auckenthaler, G. Raso, P. Huggenberger, Particle transport in a karst aquifer: natural and artificial tracer experiments with bacteria, bacteriophages and microspheres, Water Sci. Technol. 46 (3) (2002) 131–138, https://doi.org/10.2166/wst.2002.0072.
[35] F. Einsiedl, Flow system dynamics and water storage of a fissured-porous karst aquifer characterized by artificial and environmental tracers, J. Hydrol. 312 (1–4) (2005) 312–321, https://doi.org/10.1016/j.jhydrol.2005.03.031.
[36] L. Savoy, Use of Natural and Artificial Reactive Tracers to Investigate the Transfer of Solutes in Karst Systems, Diss., Université de Neuchâtel, 2007.
[37] L. Palcsu, A. Gessert, M. Túri, A. Kovács, I. Futó, J. Orsovszki, A. Puskás-Preszner, M. Temovski, G. Koltai, Long-term time series of environmental tracers reveal recharge and discharge conditions in shallow karst aquifers in Hungary and Slovakia, J. Hydrol. Reg. Stud. 36 (2021) 100858, https://doi.org/10.1016/j.ejrh.2021.100858.
[38] M. Sprenger, T.H.M. Volkmann, T. Blume, M. Weiler, Estimating Flow and Transport Parameters in the Unsaturated Zone with Pore Water Stable Isotopes, vol. 9, 2015, pp. 2617–2635, https://doi.org/10.5194/hess-19-2617-2015.
[39] D. Fronzi, F. Mirabella, C. Cardellini, S. Caliro, S. Palpacelli, C. Cambi, D. Valigi, A. Tazioli, The role of faults in groundwater circulation before and after seismic events: insights from tracers, water isotopes and geochemistry, Water 13 (11) (2021) 1499, https://doi.org/10.3390/w13111499.
[40] B. Guo, F. Yang, J. Fan, Y. Lu, The changes of spatiotemporal pattern of rocky desertification and its dominant driving factors in typical karst mountainous areas under the background of global change, Rem. Sens. 14 (10) (2022) 2351, https://doi.org/10.3390/rs14102351.
[41] B. De la Torre, J.M. Gil-Márquez, M. Mudarra, B. Andreo, Towards a better understanding of flow-related processes in the vertically distributed compartments of karst aquifers by combining natural tracers and stable isotopes, J. Hydrol. 620 (2023) 129392, https://doi.org/10.1016/j.jhydrol.2023.129392.
[42] N. Goldscheider, J. Meiman, M. Pronk, C. Smart, Tracer tests in karst hydrogeology and speleology, Int. J. Speleol. 37 (1) (2008) 27–40.
[43] M. Filippini, G. Squarzoni, J. De Waele, A. Fiorucci, B. Vigna, B. Grillo, A. Riva, S. Rossetti, L. Zini, G. Casagrande, C. Stumpp, A. Gargini, Differentiated spring behavior under changing hydrological conditions in an alpine karst aquifer, J. Hydrol. 556 (2018) 572–584, https://doi.org/10.1016/j.jhydrol.2017.11.040.
[44] S. Frank, N. Goepper, N. Goldscheider, Field tracer tests to evaluate transport properties of tryptophan and humic acid in karst, Ground Water 59 (1) (2021) 59–70.
[45] E. Patacca, R. Sartori, P. Scandone, Tyrrhenian Basin and Apennines. Kinematic Evolution and Related Dynamic Constraints, Recent Evolution and Seismicity of the Mediterranean Region, 1993, pp. 161–171.
[46] F. Ghisetti, L. Vezzani, Depth and modes of pliocene–pleistocene crustal extension of the Apennines (Italy), Terra. Nova 11 (2-3) (1999) 67–72, https://doi.org/10.1046/j.1365-3121.1999.00227.x.
[47] R. Sartori, L. Torelli, N. Zitellini, G. Carrara, M. Magaldi, P. Mussoni, Crustal features along a W–E tyrrhenian transect from Sardinia to Campania margins (central Mediterranean), Tectonophysics 383 (3–4) (2004) 171–192.
[48] V. Acocella, R. Funiciello, Transverse systems along the extensional Tyrrhenian margin of central Italy and their influence on volcanism, Tectonics 25 (2) (2006), https://doi.org/10.1029/2005TC001845.
[49] E. Carminati, S. Fabbi, M. Santantonio, Slab bending, syn-subduction normal faulting, and out-of-sequence thrusting in the Central Apennines, Tectonics 33 (4) (2014) 530–551, https://doi.org/10.1002/2013TC003386.
[50] A. Beaudoin, R. Augier, L. Jolivet, A. Jourdon, H. Raimbourg, S. Scaillet, G.L. Cardello, Deformation behavior of continental crust during subduction and exhumation: strain distribution over the Tenda massif (Alpine Corsica, France), Tectonophysics 705 (2017) 12–32, https://doi.org/10.1016/j.tecto.2017.03.023.
[51] G.L. Cardello, C. Doglioni, From mesozoic rifting to Apennine orogeny: the gran Sasso range (Italy), Gondwana Res. 27 (4) (2015) 1307–1334, https://doi.org/10.1016/j.gr.2014.09.009.
[52] G.L. Cardello, L. Tomassetti, I. Cornacchia, A. Mancini, M. Mancini, I. Mazzini, G. Rusciadelli, E. Capezzuoli, V. Lorenzi, M. Petitta, G.P. Cavinato, O. Girotti, M. Brandano, The Tethyan and Tyrrhenian margin record of the Central Apennines: a guide with insights from stratigraphy, tectonics, and hydrogeology, GFT&M. 14 (2.2) (2022) 1–113.
[53] F. Ghisetti, L. Vezzani, Interfering paths of deformation and development of arcs in the fold-and-thrust belt of the central Apennines (Italy), Tectonics 16 (3) (1997) 523–536.
[54] S. Bigi, P. Casero, G. Ciotoli, Seismic interpretation of the Laga basin; constraints on the structural setting and kinematics of the Central Apennines, J. Geol. Soc. 168 (1) (2011) 179–190.
[55] G.P. Cavinato, P.D. Celles, Extensional basins in the tectonically bimodal central Apennines fold-thrust belt, Italy: response to corner flow above a subducting slab in retrograde motion, Geology 27 (10) (1999) 955–958, https://doi.org/10.1130/0091-7613(1999)027<0955:EBITTB>2.3.CO;2.
[56] N. D'Agostino, N. Chamot-Rooke, R. Funiciello, L. Jolivet, F. Speranza, The role of pre-existing thrust faults and topography on the styles of extension in the Gran Sasso range (central Italy), Tectonophysics 292 (3–4) (1998) 229–254, https://doi.org/10.1016/S0040-1951(98)00070-5.
[57] M. Tallini, R. Adinolfi Falcone, V. Carucci, A. Falgiani, B. Parisse, M. Petitta, Isotope hydrology and geochemical modeling: new insights into the recharge processes and water–rock interactions of a fissured carbonate aquifer (Gran Sasso, central Italy), Environ. Earth Sci. 72 (2014) 4957–4971, https://doi.org/10.1007/s12665-014-3364-9.
[58] M. Barbieri, T. Boschetti, M. Petitta, M. Tallini, Stable isotope (2H, 18O and 87Sr/86Sr) and hydrochemistry monitoring for groundwater hydrodynamics analysis in a karst aquifer (Gran Sasso, Central Italy), Appl. Geochem. 20 (2005) 2063–2081, https://doi.org/10.1016/j.apgeochem.2005.07.008.
[59] M. Tallini, B. Parisse, M. Petitta, M. Spizzico, Long-term spatio-temporal hydrochemical and 222Rn tracing to investigate groundwater flow and water–rock interaction in the Gran Sasso (central Italy) carbonate aquifer, Hydrogeol. J. 21 (2013) 1447–1467, https://doi.org/10.1007/s10040-013-1023-y.
[60] F. Ghisetti, L. Vezzani, Thrust belt development in the central Apennines (Italy): northward polarity of thrusting and out-of-sequence deformations in the Gran Sasso Chain, Tectonics 10 (5) (1991) 904–919.

[61] S. Bigi, F. Calamita, E. Centamore, Caratteristiche geologico-strutturali dell'area abruzzese ad oriente del Gran Sasso, Studi Geol. Camerti 2 (1995) 67–76.
[62] S. Bigi, F. Calamita, G. Cello, E. Centamore, G. Deiana, W. Paltrinieri, P.P. Pierantoni, M. Ridolfi, Tectonics and sedimentation within a messinian foredeep in the central Apennines, Italy, J. Petrol. Geol. 22 (1999) 5–18, https://doi.org/10.1111/j.1747-5457.1999.tb00456.x.
[63] M. Petitta, M. Tallini, Idrodinamica sotterranea del massiccio del Gran Sasso (Abruzzo): Nuove indagini idrologiche, idrogeologiche e idrochimiche (1994–2001), Boll. Della Soc. Geol. Ital. 121 (3) (2002) 343–363.
[64] G. Medici, V. Lorenzi, C. Sbarbati, M. Manetta, M. Petitta, Structural classification, discharge statistics, and recession analysis from the springs of the Gran Sasso (Italy) carbonate aquifer; Comparison with selected analogues worldwide, Sustainability 15 (13) (2023) 10125, https://doi.org/10.3390/su151310125.
[65] E. Centamore, G. Deiana, F. Calamita, S. Bigi, M. Ridolfi, R. Salvucci, Assetto strutturale e cronologia della deformazione della zona d'incontro tra il dominio umbro-marchigiano e laziale-abruzzese, Studi Geologici Camerti, CROP 11 (1991) 2.
[66] S. Milli, C. D'Ambrogi, P. Bellotti, G. Calderoni, M.G. Carboni, A. Celant, L. Di Bella, F. Di Rita, V. Frezza, D. Magri, R.M. Pichezzi, V. Ricci V, The transition from wave-dominated estuary to wave-dominated delta: the Late Quaternary stratigraphic architecture of Tiber River deltaic succession (Italy), Sediment. Geol. 284 (2013) 159–180.
[67] L. Ferracuti, G. Marinelli, S. Rusi, Idrogeologia e monitoraggio delle sorgenti carsiche del Tavo (massiccio carbonatico del Gran Sasso) e loro implicazioni nella gestione dell'emergenza torbidità, G. Geol. (Bologna) 3 (2006) 47–52, https://doi.org/10.1474/GGA.2006-03.0-06.0099.
[68] A. Monjoie, in: Livre Jubilaire, L. Calembert (Eds.), Prévision et contrôle des caractéristiques Hydrogéologiques dans les tunnels du Gran Sasso (Apennin-Italie), Thone, 1980, pp. 209–229.
[69] P. Celico, S. Fabbrocino, M. Petitta, M. Tallini, Hydrogeological impact of the Gran Sasso motor-way tunnels (Central Italy), G. Geol. Appl. 1 (2005) 157–165, https://doi.org/10.1474/GGA.2005-01.0-16.0016.
[70] A. Amoruso, L. Crescentini, M. Petitta, S. Rusi, M. Tallini, Impact of the 6 April 2009 L'Aquila earthquake on groundwater flow in the Gran Sasso carbonate aquifer, Central Italy, Hydrol. Process. 25 (2011) 1754–1764, https://doi.org/10.1002/hyp.7933.
[71] R. Adinolfi Falcone, V. Carucci, A. Falgiani, M. Manetta, B. Parisse, M. Petitta, S. Rusi, M. Spizzico, M. Tallini, Changes on groundwater flow and hydrochemistry of the Gran Sasso carbonate aquifer after 2009 L' Aquila earthquake, Ital. J. Geosci. 131 (2012) 459–474, https://doi.org/10.3301/IJG.2011.34.
[72] A. Amoruso, L. Crescentini, M. Petitta, M. Tallini, Parsimonious recharge/discharge modeling in carbonate fractured aquifers: the groundwater flow in the Gran Sasso aquifer (Central Italy), J. Hydrol. 476 (2013) 136–146, https://doi.org/10.1016/j.jhydrol.2012.10.026.
[73] A. Amoruso, L. Crescentini, S. Martino, M. Petitta, M. Tallini, Correlation between groundwater flow and deformation in the fractured carbonate Gran Sasso aquifer (INFN underground laboratories, central Italy), Water Resour. Res. 50 (2014) 4858–4876, https://doi.org/10.1002/2013WR014491.
[74] L. Siegel, N. Goldscheider, M. Petitta, J. Xanke, B. Andreo, M. Bakalowicz, J.A. Barberá, R. Bouhlila, A. Burg, J. Doummar, I. Ezzine, J. Fernández-Ortega, M. Ghanmi, H. Jourde, A.I. Marín, A. Mhimdi, T. Pipan, N. Ravbar, A. Maran Stevanović, Z. Stevanović, Distribution, threats and protection of selected karst groundwater-dependent ecosystems in the Mediterranean region, Hydrogeol. J. 31 (2023) 2231–2249, https://doi.org/10.1007/s10040-023-02711-9.
[75] S. Rusi, G. Marinelli, The problem of turbidity in the management of karstic springs: the example of Tavo springs (gran Sasso carbonate massif, Central Italy). Proceedings of the International Conference on Water Resources & Environmental Problems in Karst, Belgrade and Kotor, 2005, pp. 525–530.
[76] P.A. Schnegg, An Inexpensive Field Fluorometer for Hydrogeological Tracer Tests with Three Tracers and Turbidity Measurement, Articles of the Geomagnetism Group at the University of Neuchâtel, Groundwater and Human Development, 2002, pp. 1484–1488.
[77] P.A. Schnegg, L. Thueler, Application of a Multi-LED Field Fluorometer for Simultaneous Detection of Hard to Separate Dye Tracers and Fluocapteurs, 11th Conference of Latin American hydrogeology, 2012.
[78] I. Clark, Groundwater Geochemistry and Isotopes, CRC press, 2015.
[79] M. Petitta, F. Banzato, V. Lorenzi, E. Matani, C. Sbarbati, Determining recharge distribution in fractured carbonate aquifers in central Italy using environmental isotopes: snowpack cover as an indicator for future availability of groundwater resources, Hydrogeol. J. 30 (5) (2022) 1619–1636, https://doi.org/10.1007/s10040-022-02501-9.
[80] V. Lorenzi, M.D. Barberio, C. Sbarbati, M. Petitta, Groundwater recharge distribution due to snow cover in shortage conditions (2019–22) on the Gran Sasso carbonate aquifer (Central Italy), Environ. Earth Sci. 82 (9) (2023) 1–15, https://doi.org/10.1007/s12665-023-10889-0.
[81] V. Vincenzi, A. Gargini, N. Goldscheider, Using tracer tests and hydrological observations to evaluate effects of tunnel drainage on groundwater and surface waters in the Northern Apennines (Italy), Hydrogeol. J. 17 (1) (2009) 135–150.
[82] H. Behrens, U. Beims, H. Dieter, G. Dietze, T. Eikmann, T. Grummt, H. Hanisch, H. Henseling, W. Käß, H. Kerndorff, C. Leibundgut, U. Müller-Wegener, I. Rönnefahrt, B. Scharenberg, R. Schleyer, W. Schloz, F. Tilkes, Toxicological and ecotoxicological assessment of water tracers, Hydrogeol. J. 9 (2001) 321–325, https://doi.org/10.1007/s100400100126.
[83] W. Käss, in: G. Matthess (Ed.), Geohydrologische Markierungstechnik [Textbook of Geohydrological Marking and Tracing Techniques], Lehrbuch der Hydrogeologie vol. 9, 2004.
[84] C.J. Taylor, E.A. Greene, Hydrogeologic Characterization and Methods Used in the Investigation of Karst Hydrology, Field Techniques for Estimating Water Fluxes between Surface Water and Ground Water, 2008, pp. 75–114.
[85] R. Benischke, N. Goldscheider, C. Smart, in: N. Goldscheider, D. Drew (Eds.), Tracer techniques, Methods in Karst Hydrogeology, Taylor and Francis, London, 2007, pp. 147–170.
[86] L. Palcsu, A. Gessert, M. Túri, A. Kovács, I. Futó, J. Orsovszki, A. Puskás-Preszner, M. Temovski, G. Koltai, Long-term time series of environmental tracers reveal recharge and discharge conditions in shallow karst aquifers in Hungary and Slovakia, J. Hydrol. Reg. Stud. 36 (2021) 100858, https://doi.org/10.1016/j.ejrh.2021.100858.
[87] Z. Kattan, Environmental isotope study of the major karst springs in Damascus limestone aquifer systems: case of the Figeh and Barada springs, J. Hydrol. 193 (1–4) (1997) 161–182, https://doi.org/10.1016/S0022-1694(96)03137-X.
[88] N.N. Ozyurt, H.O. Lutz, T. Hunjak, D. Mance, Z. Roller-Lutz, Characterization of the Gacka River basin karst aquifer (Croatia): hydrochemistry, stable isotopes and tritium-based mean residence times, Sci. Total Environ. 487 (2014) (2014) 245–254.
[89] N. Toride, F.J. Leij, M.T. Van Genuchten, The CXTFIT Code for Estimating Transport Parameters from Laboratory or Filed Tracer Experiments, vol. 2, US Salinity Laboratory, Riverside, CA, 1995.
[90] L. Calambert, P.G. Catalano, V. Conato, L. Lambrecht, A. Monjoie, Observations dans le massif du Gran Sasso (Apennin central), C.R. Acad. Sc., Paris, 1972, p. 274.
[91] A. Monjoie, Hydrogeologie du massif du Gran Sasso, Appenin Central), 1975.
[92] P.G. Catalano, G.P. Cavinato, F. Salvini, M. Tozzi, Analisi Strutturale nei laboratori dell'I.N.F.N. del Gran Sasso d'Italia, Boll. Soc. Geol. It. 35 (1986) 647–655.